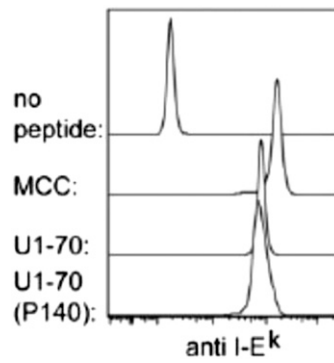
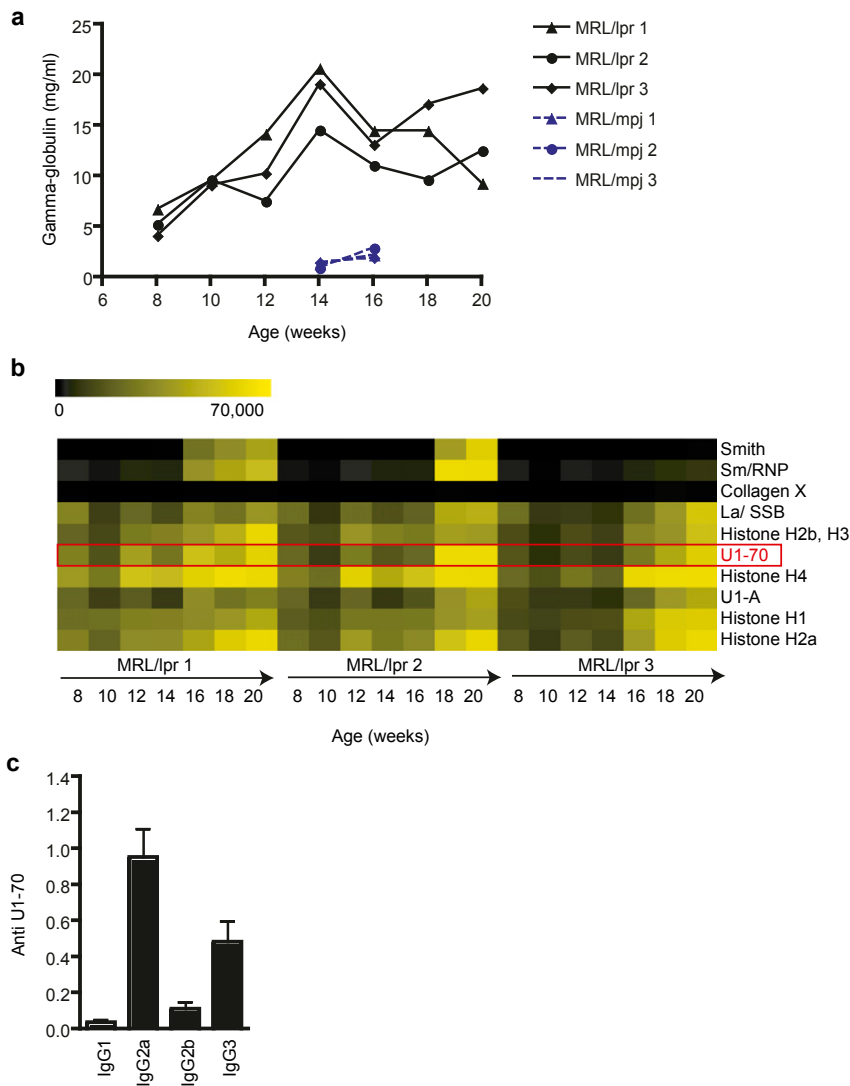


# Supporting Information

Kattah et al. 10.1073/pnas.1424796112



**Fig. S1.** U1-70 peptides form stable peptide:MHC complexes with I-E<sup>k</sup>. Shown are histograms from flow cytometry staining of exchanged, biotinylated peptide:I-E<sup>k</sup> complexes, incubated with streptavidin beads and stained with anti-I-E<sup>k</sup> (PE), demonstrating that exchanged monomers are stable.



**Fig. S2.** Autoantibody production in MRL/lpr mice. (A) Levels of gamma globulin were measured in the serum of 3 MRL/lpr and 3 MRL/mpj mice, bled at 2-wk intervals for 12 wk, and detected by ELISA. (B) Heat map of antigens identified by SAM as having a statistically significant association with MRL/lpr serum from mice aged >15 wk vs. serum from mice aged <15 wk. Data are derived from autoantigen microarrays probed with individual mouse serum samples. The heat map represents a gradient from low (pseudocolored black) to high (pseudocolored yellow) IgG levels. (C) Levels of autoantibodies against U1-70 of various IgG isotypes, as measured by ELISA ( $n = 3$  mice).

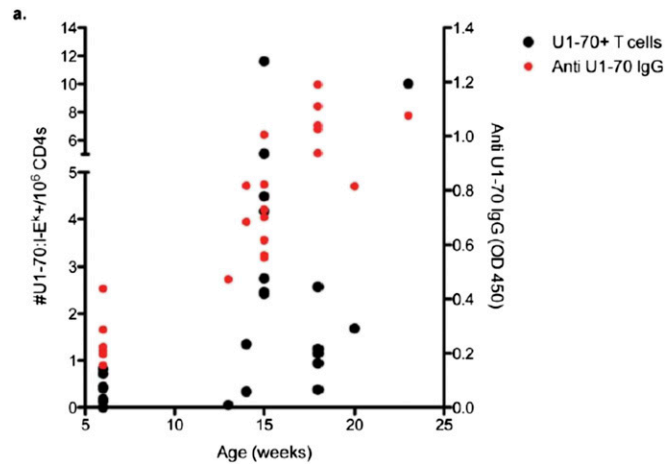


**Fig. S3.** Kinetics of U1-70:I-E<sup>k</sup>-specific T cells and anti-U1-70 autoantibodies. Frequencies of U1-70:I-E<sup>k</sup>-specific T cells (*Left y axis*) were determined based on the number of tetramer-positive cells detected following enrichment. The levels of IgG autoantibodies against the whole protein U1-70 in sera from MRL/lpr mice were measured by ELISA (*Right y axis*), and graphed alongside the frequency of U1-70:I-E<sup>k</sup>-specific T cells.

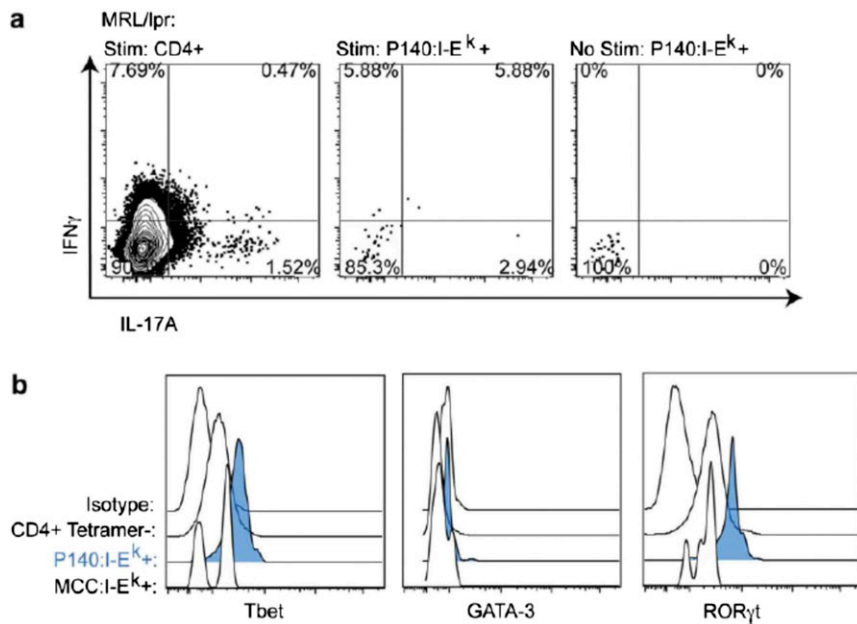


**Fig. S4.** P140:I-E<sup>k</sup>-specific T-cell phenotype. (A) Flow cytometry plots showing intracellular IL-17 and IFN $\gamma$  production by MRL/lpr CD4<sup>+</sup> T cells, stimulated with PMA/ionomycin for 3 h at 37 °C. The plots show the enrichment fraction and are gated on CD4<sup>+</sup> P140:I-E<sup>k</sup>-negative cells (*Left*), CD4<sup>+</sup> P140:I-E<sup>k</sup>-positive cells (*Middle*), and CD4<sup>+</sup> P140:I-E<sup>k</sup>-positive cells that were not stimulated (*Right*). (B) Histograms of ROR $\gamma$ t, Tbet, and GATA3 expression from tetramer-enriched MRL/lpr CD4<sup>+</sup> T cells, as measured by intracellular staining.

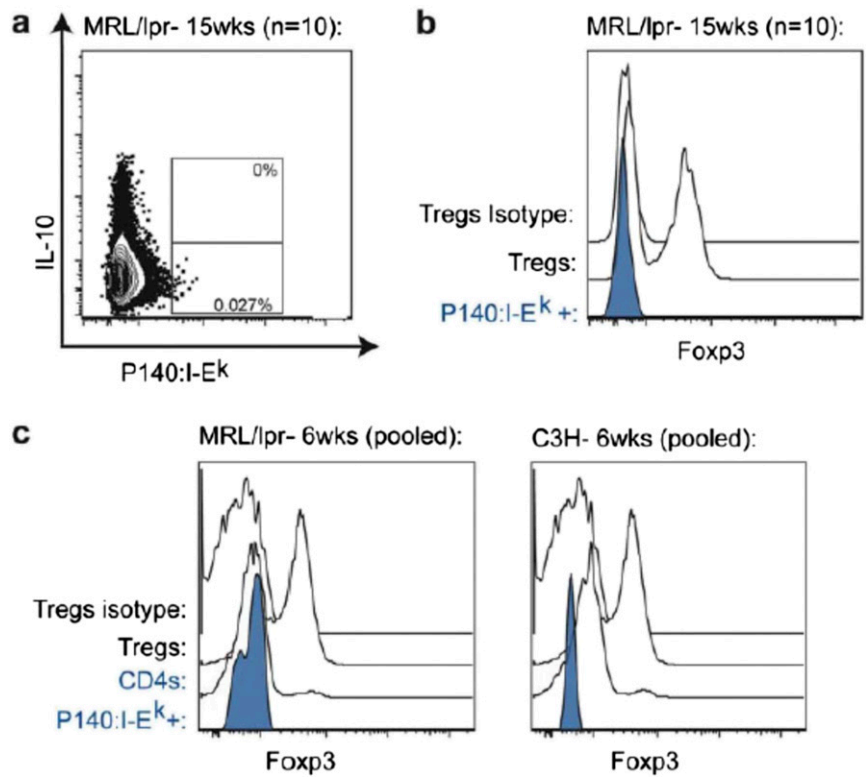


**Fig. S5.** P140:I-E<sup>k</sup>-specific T cells do not express Treg markers. (A and B) Flow cytometry plots of CD4<sup>+</sup> T cells from MRL/lpr mice at age 15 wk, stimulated with PMA/ionomycin for 3 h at 37 °C, and stained for IL-10 (A) and Foxp3 (B). Plots are representative of 10 individual mice. (C) Foxp3 expression was measured in 6-wk-old MRL/lpr (Left) and C3H (Right) mice. Five mice were pooled for each sample. As a positive control, Foxp3 expression was detected in CD4<sup>+</sup> T cells from MRL/lpr mice that were purified by negative selection, cultured with TGFβ, and gated on CD25<sup>hi</sup>, CD127<sup>lo</sup>.

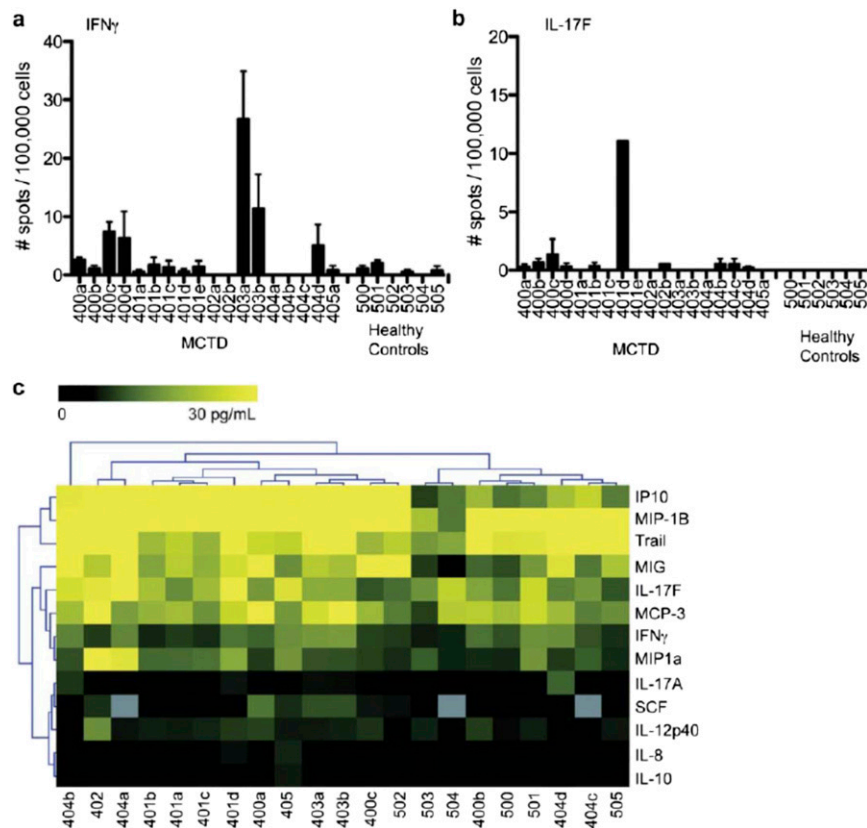


**Fig. S6.** Cytokine levels in MCTD patients. (A and B) Bar graphs showing IFN $\gamma$  (A) and IL-17F (B) production from MCTD patient samples in response to the U1-70 peptide, as detected by ELISPOT assays. Error bars reflect triplicate wells. Age- and sex-matched healthy controls were included. (C) Heat map of unsupervised hierarchical clustering of soluble factors identified by SAM as having a statistically significant association with MCTD patient serum vs. healthy control serum. Data are derived from a Luminex assay and are the average values from triplicate wells.

**Table S1. Candidate peptide panel for I-E<sup>k</sup> tetramers**

Test	Protein	Amino acids	Sequence	Source
* $\Delta$ $\diamond$	B2M	42–59	HPHIEIQLMKNKGKIPK	(1)
* $\Delta$ $\diamond$	Histone H2A	84–99	HLQLAIRNDEELNKLGGKVT	(1)
* $\Delta$	Histone H2A	84–99 E94N	HLQLAIRNDENLNKLGGKVT	Mutation made based on MHC prediction
$\Delta$	Histone H3	20–40	RKSTFFKAPRKQLATKAARK	MHC prediction
$\Delta$	Histone H4	60–80	VFLENVIRDAVITYTEHAKRK	MHC prediction
$\Delta$	La	50–70	IMIKFNRLNRLTDFNVIVE	MHC prediction
$\Delta$	Ro52	1–20	MASAARLTMWEEVTCPICL	MHC prediction
$\Delta$	Ro52	210–230	LGEKEAKLAQQSQALQELIS	MHC prediction
* $\Delta$	Ro60	272–287	LLQEMPLTALLRNLGK	MHC prediction
* $\Delta$	Ro60	272–287 T297I	LLQEMPLIALLRNLGK	Mutation made based on MHC prediction
* $\Delta$ $\diamond$	Srp20	4–23	DSCPLDCKVYVGNLGNNGNK	(1)
* $\Delta$	Srp20	4–23 N22K	DSCPLDCKVYVGNLGNNGKK	Mutation made based on MHC prediction
* $\Delta$ $\diamond$	U1-70	131–151	RIHMOVYSKRSKGKPRGYAFIE	(2)
*	U1-70	131–151 (P140)	RIHMOVYSKRS(phospho) GKPRG YAFIE	(2)
$\Delta$	U1-A	610–630	DIAFVFEFDNEVQAGAARDAL	MHC prediction

Candidate peptides or whole antigens were tested for binding to I-E<sup>k</sup> by competition assay (\*), and/or for the ability to induce proliferation of CD4<sup>+</sup> T cells from MRL/lpr mice by <sup>3</sup>H thymidine incorporation ( $\Delta$ ), or the up-regulation of CD40L on CD4<sup>+</sup> T cells as measured by flow cytometry ( $\diamond$ ).

- Muller S, et al. (2008) Spliceosomal peptide P140 for immunotherapy of systemic lupus erythematosus: Results of an early phase II clinical trial. *Arthritis Rheum* 58(12):3873–3883.
- Tusher VG, Tibshirani R, Chu G (2001) Significance analysis of microarrays applied to the ionizing radiation response. *Proc Natl Acad Sci USA* 98(9):5116–5121.